TELKOMNIKA, Vol. 11, No. 4, April 2013, pp. 2058~2063
ISSN: 2302-4046

Semi-implicit Image Denoising Algorithm for Different Boundary Conditions

Yuying Shi*[1], Yonggui Zhu[2], Jingjing Liu[1]
[1]Department of Mathematics and Physics, North China Electric Power University Beijing, China
[2]School of Science, Communication University of China, Beijing, China
*Corresponding author, e-mail: yyshi@amss.ac.cn

Abstract

In this paper, the Crank-Nicolson semi-implicit difference scheme in matrix form is applied to discrete the Rudin-Osher-Fatemi model. We also consider five kinds of different boundary conditions: Dirichlet boundary conditions, periodic boundary conditions, Neumann boundary conditions, antireflective boundary conditions and mean boundary conditions. By comparing the experimental results of Crank-Nicolson semi-implicit scheme and explicit scheme with the proposed boundary conditions, we can get that the semi-implicit scheme can overcome the instability and the number of iterations of the shortcomings that the explicit discrete scheme has, and its recovery effects are better than the explicit discrete scheme. In addition, the antireflective boundary conditions and Neumann boundary conditions can better maintain the continuity of the boundary in image denoising.

Keywords: *denoising, Rudin-Osher-Fatemi model, Crank-Nicolson difference scheme, boundary conditions, mean boundary conditions*

1. Introduction

Image denoising is to keep the useful information and reduces or eliminates the interference and noise of the image. The Rudin-Osher-Fatemi (ROF) model [1] used the total variation (TV) norm as a regularization function, which does not penalize the discontinuity in u, and thus allows us to recover the edges of the original image. The ROF model is as follows:

$$u_t = \nabla\left(\frac{\nabla u}{|\nabla u|_\beta}\right) - \lambda * (u - f), \tag{1}$$

with $u(x,0)$ given as initial data. The parameter $\lambda > 0$ is a balancing factor and $\beta > 0$ is a small regularization parameter.

The corresponding Euler-Lagrange equation of the ROF model is usually solved by the explicit scheme [2], but the explicit scheme converges slowly. The Crank-Nicolson (C-N) difference scheme [3] is a second-order method in time and unconditionally stable. One research tendency addresses image processing algorithms. Kim used the C-N difference scheme to solve the ROF model by the point-by-point method [4]. Wang et al. combined the C-N difference scheme with the fixed point method to discrete the ROF model [5]. The experimental results demonstrated that the semi-implicit discrete scheme has fewer iterative numbers than the ones of the explicit discrete scheme, and the denoised results are better than that of the explicit discrete scheme with the same iterative numbers. But they only considered the case of Neumann boundary conditions (BCs). Kim et al. adopted a linearized C-N alternating direction implicit time-stepping procedure to simulate the PDE-based model efficiently [6]. The semi-implicit C-N scheme was introduced in [7] based on locally one-dimensional (LOD)/ additive operator splitting (AOS) for implementing the anisotropic Beltrami operator. Niang et al. also proposed an approach based on partial differential equations with C-N scheme, also showed its efficiency in signal and image processing [8]. Sun et al. proposed an improved 2-D maximum entropy algorithm and applied it in lettuce object segmentation [9]. Swastika presented the simulation of compressed sensing for Thoracic MR imaging with

Received January 8, 2013; Revised February 22, 2013; Accepted March 4, 2013

circulant matrices as the sensing matrices [10]. The simulation results showed that the circulant matrices work efficiently for sparse image in the spatial domain.

In the process of calculating the difference scheme, several kinds of BCs [11] need to be considered such as Dirichlet BCs, periodic BCs, Neumann BCs, antireflective BCs and mean BCs. To make out the difference among different kinds of BCs, assume a signal in one dimensional space

$$\tilde{U}=(\cdots,\ u_{-m+1},\ \cdots,\ u_0,\ u_1,\ \cdots,\ u_n,\ u_{n+1},\ \cdots,)^T, \tag{2}$$

as an example. Let

$$u_l=\begin{pmatrix} u_{-m+1} \\ \vdots \\ u_{-1} \\ u_0 \end{pmatrix}, u=\begin{pmatrix} u_1 \\ \vdots \\ u_{n-1} \\ u_n \end{pmatrix}, u_r=\begin{pmatrix} u_{n+1} \\ \vdots \\ u_{n+m-1} \\ u_{n+m} \end{pmatrix}. \tag{3}$$

The denoised result is affected not only by $u=\left(u(1),\ \cdots,\ u(n)\right)^T$ but also by $\left(u(-m+1),\ \cdots,\ u(0)\right)^T$ and $\left(u(n+1),\ \cdots,\ u(n+m)\right)^T$. For the different boundary values u_l and u_r with different kinds of BCs, we refer the reader to [11] for details.

In this paper, we will apply the Crank-Nicolson semi-implicit difference scheme in matrix form to solve the ROF model with the five kinds of BCs. Section 2 presents the different matrices formed by the five kinds of BCs which are used in the semi-implicit algorithm. Section 3 shows some experimental results. Some conclusions are given in section 4.

2. A Semi-implicit Algorithm

In this section, we will show a semi-implicit algorithm to solve Equation (1). Let $u_{i,j}^n$ be an approximation of $u(x_i,y_j,t_n)$, where $x_i=i\Delta x,\ y_j=j\Delta y,\ t_n=n\Delta t,\ n\geq 1$. Let $s_{i,j}^n=u_{i,j}^{xx}((u_{i,j}^y)^2+\beta)-2u_{i,j}^{xy}u_{i,j}^x u_{i,j}^y+u_{i,j}^{yy}((u_{i,j}^x)^2+\beta)$ and $v_{i,j}^n=((u_{i,j}^x)^2+(u_{i,j}^y)^2+\beta)^{3/2}$. By the C-N difference scheme, Eq. (3) is discretized into:

$$(1+\frac{1}{2}*\lambda*\Delta t)*u_{i,j}^{n+1}-\frac{1}{2}*\Delta t*\frac{s_{i,j}^{n+1}}{v_{i,j}^n}=u_{i,j}^n+\Delta t*(\frac{1}{2}*\frac{s_{i,j}^n}{v_{i,j}^n}-\frac{1}{2}*\lambda*u_{i,j}^n+\lambda*u_{i,j}^0), \tag{4}$$

with $u_{i,j}^0$ as an initial value, and the definition of the derivative terms is the same as [12]. Then u can be calculated by the point-to-point calculating method.

Following the idea of [5], the second derivatives of U can be rewritten as the product of some tri-diagonal matrices and the matrix U. To show the relation between the second derivatives U^{xx}, U^{yy}, U^{xy} and the image matrix U, we give an example with $U_{5\times 5}$ matrix and let $\Delta x,\ \Delta y$ be the step size as follows.

(1)The matrices in Dirichlet BCs:

$$U^{xx}=\frac{D_1*U}{(\Delta x)^2}=\begin{pmatrix} -2 & 1 & 0 & 0 & 0 \\ 1 & -2 & 1 & 0 & 0 \\ 0 & 1 & -2 & 1 & 0 \\ 0 & 0 & 1 & -2 & 1 \\ 0 & 0 & 0 & 1 & -2 \end{pmatrix}\begin{pmatrix} u_{11} & u_{12} & u_{13} & u_{14} & u_{15} \\ u_{21} & u_{22} & u_{23} & u_{24} & u_{25} \\ u_{31} & u_{32} & u_{33} & u_{34} & u_{35} \\ u_{41} & u_{42} & u_{43} & u_{44} & u_{45} \\ u_{51} & u_{52} & u_{53} & u_{54} & u_{55} \end{pmatrix};$$

$$U^{xy}=\frac{E_1*U*F_1}{4(\Delta x)(\Delta y)}=\frac{1}{4}\begin{pmatrix}0&1&0&0&0\\-1&0&1&0&0\\0&-1&0&1&0\\0&0&-1&0&1\\0&0&0&-1&0\end{pmatrix}\begin{pmatrix}u_{11}&u_{12}&u_{13}&u_{14}&u_{15}\\u_{21}&u_{22}&u_{23}&u_{24}&u_{25}\\u_{31}&u_{32}&u_{33}&u_{34}&u_{35}\\u_{41}&u_{42}&u_{43}&u_{44}&u_{45}\\u_{51}&u_{52}&u_{53}&u_{54}&u_{55}\end{pmatrix}\begin{pmatrix}0&-1&0&0&0\\1&0&-1&0&0\\0&1&0&-1&0\\0&0&1&0&-1\\0&0&0&1&0\end{pmatrix};$$

$$U^{yy}=\frac{U*G_1}{(\Delta y)^2}=\begin{pmatrix}u_{11}&u_{12}&u_{13}&u_{14}&u_{15}\\u_{21}&u_{22}&u_{23}&u_{24}&u_{25}\\u_{31}&u_{32}&u_{33}&u_{34}&u_{35}\\u_{41}&u_{42}&u_{43}&u_{44}&u_{45}\\u_{51}&u_{52}&u_{53}&u_{54}&u_{55}\end{pmatrix}\begin{pmatrix}-2&1&0&0&0\\1&-2&1&0&0\\0&1&-2&1&0\\0&0&1&-2&1\\0&0&0&1&-2\end{pmatrix}.$$

(2)The matrices in periodic BCs:

$$U^{xx}=\frac{D_2*U}{(\Delta x)^2}=\begin{pmatrix}-2&1&0&0&1\\1&-2&1&0&0\\0&1&-2&1&0\\0&0&1&-2&1\\1&0&0&1&-2\end{pmatrix}\begin{pmatrix}u_{11}&u_{12}&u_{13}&u_{14}&u_{15}\\u_{21}&u_{22}&u_{23}&u_{24}&u_{25}\\u_{31}&u_{32}&u_{33}&u_{34}&u_{35}\\u_{41}&u_{42}&u_{43}&u_{44}&u_{45}\\u_{51}&u_{52}&u_{53}&u_{54}&u_{55}\end{pmatrix};$$

$$U^{xy}=\frac{E_2*U*F_2}{4(\Delta x)(\Delta y)}=\frac{1}{4}\begin{pmatrix}0&1&0&0&-1\\-1&0&1&0&0\\0&-1&0&1&0\\0&0&-1&0&1\\1&0&0&-1&0\end{pmatrix}\begin{pmatrix}u_{11}&u_{12}&u_{13}&u_{14}&u_{15}\\u_{21}&u_{22}&u_{23}&u_{24}&u_{25}\\u_{31}&u_{32}&u_{33}&u_{34}&u_{35}\\u_{41}&u_{42}&u_{43}&u_{44}&u_{45}\\u_{51}&u_{52}&u_{53}&u_{54}&u_{55}\end{pmatrix}\begin{pmatrix}0&-1&0&0&1\\1&0&-1&0&0\\0&1&0&-1&0\\0&0&1&0&-1\\-1&0&0&1&0\end{pmatrix};$$

$$U^{yy}=\frac{U*G_2}{(\Delta y)^2}=\begin{pmatrix}u_{11}&u_{12}&u_{13}&u_{14}&u_{15}\\u_{21}&u_{22}&u_{23}&u_{24}&u_{25}\\u_{31}&u_{32}&u_{33}&u_{34}&u_{35}\\u_{41}&u_{42}&u_{43}&u_{44}&u_{45}\\u_{51}&u_{52}&u_{53}&u_{54}&u_{55}\end{pmatrix}\begin{pmatrix}-2&1&0&0&1\\1&-2&1&0&0\\0&1&-2&1&0\\0&0&1&-2&1\\1&0&0&1&-2\end{pmatrix}.$$

(3) The matrices in Neumann BCs can be found in [5]. We denote the corresponding matrices D_3, E_3, F_3, G_3.

(4)The matrices in antireflective BCs:

$$U^{xx}=\frac{D_4*U}{(\Delta x)^2}=\begin{pmatrix}0&0&0&0&0\\1&-2&1&0&0\\0&1&-2&1&0\\0&0&1&-2&1\\0&0&0&0&0\end{pmatrix}\begin{pmatrix}u_{11}&u_{12}&u_{13}&u_{14}&u_{15}\\u_{21}&u_{22}&u_{23}&u_{24}&u_{25}\\u_{31}&u_{32}&u_{33}&u_{34}&u_{35}\\u_{41}&u_{42}&u_{43}&u_{44}&u_{45}\\u_{51}&u_{52}&u_{53}&u_{54}&u_{55}\end{pmatrix};$$

$$U^{xy}=\frac{E_4*U*F_4}{4(\Delta x)(\Delta y)}=\frac{1}{4}\begin{pmatrix}2&-2&0&0&0\\1&0&-1&0&0\\0&1&0&-1&0\\0&0&1&0&-1\\0&0&0&2&-2\end{pmatrix}\begin{pmatrix}u_{11}&u_{12}&u_{13}&u_{14}&u_{15}\\u_{21}&u_{22}&u_{23}&u_{24}&u_{25}\\u_{31}&u_{32}&u_{33}&u_{34}&u_{35}\\u_{41}&u_{42}&u_{43}&u_{44}&u_{45}\\u_{51}&u_{52}&u_{53}&u_{54}&u_{55}\end{pmatrix}\begin{pmatrix}2&1&0&0&0\\-2&0&1&0&0\\0&-1&0&1&0\\0&0&-1&0&2\\0&0&0&-1&-2\end{pmatrix};$$

$$U^{yy}=\frac{U*G_4}{(\Delta y)^2}=\begin{pmatrix}u_{11}&u_{12}&u_{13}&u_{14}&u_{15}\\u_{21}&u_{22}&u_{23}&u_{24}&u_{25}\\u_{31}&u_{32}&u_{33}&u_{34}&u_{35}\\u_{41}&u_{42}&u_{43}&u_{44}&u_{45}\\u_{51}&u_{52}&u_{53}&u_{54}&u_{55}\end{pmatrix}\begin{pmatrix}0&1&0&0&0\\0&-2&1&0&0\\0&1&-2&1&0\\0&0&1&-2&0\\0&0&0&1&0\end{pmatrix}.$$

For the denoising problem, only one boundary needs to be considered. Thus the mean BCs are the same as the antireflective BCs. For simplicity, we unified D_i, E_i, F_i, G_i $(i=1,2,3,4)$ as D, E, F, G. Applying the fixed point method for $\frac{s_{i,j}^{n+1}}{v_{i,j}^n}$ as in [5] and let,

$$A=\frac{((u_{i,j}^y)^2+\beta)^n}{v_{i,j}^n}, B=\frac{((u_{i,j}^x)^2+\beta)^n}{v_{i,j}^n}, C=\frac{2(u_{i,j}^x u_{i,j}^y)^n}{v_{i,j}^n}. \quad (5)$$

Thus we have:

$$\frac{s_{i,j}^{n+1}}{v_{i,j}^n}=((D*U^{n+1})\cdot*A-\frac{C}{4}\cdot*(E*U^{n+1}*F)+(U^{n+1}*G)\cdot*B)_{i,j}. \quad (6)$$

According to the same technique in [5], seven new matrices $A_1, A_2, B_1, B_2, C_1, C_2, C_3$ are constructed by A, B, C, D, E, F . Thus the three matrices dot products in (6) can be transformed into the corresponding products of the new matrices. Please refer to [5] for the details. So (4) can be rewritten as a linear equation $H_1 X^{n+1}=Y^n$, where $H_1=H_2-\frac{1}{2}*\Delta t*(A_1*A_2-C_1*C_2*C_3+B_1*B_2)$ in which H_2 is a diagonal $n^2\times n^2$ matrix whose diagonal elements are $1+\frac{1}{2}*\lambda*\Delta t$, X and Y are $n^2\times 1$ vectors. By Gauss-Seidel (G-S) iterative method, the solution vector $X_{n^2\times 1}$ is obtained. Then it is reshaped to be the denoised image $u_{n\times n}$. In this way, we need to solve a linear equation instead of the point-to-point calculation.

3. Numerical Experiments

In this section, we will show numerical results with the five different kinds of BCs--Dirichlet BCs, periodic BCs, Neumann BCs, antireflective BCs and mean BCs. The signal to noise ratio (SNR) [5] of the image u is used to measure the level of noise. Higher SNR values correspond to good denoising results. Let the space step $\Delta x=\Delta y=1$, $\beta=10$, and time step $\Delta t=0.5$.

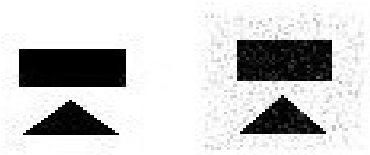

Figure 1. Original Image and Noisy Image with Gaussian Noise $\sigma=0.01$

Table 1. SNR using Dirichlet BCs

λ	explicit scheme	semi-implicit scheme
0.01	5.6963	6.6595
0.1	5.7640	6.9131
1	6.0127	6.7082

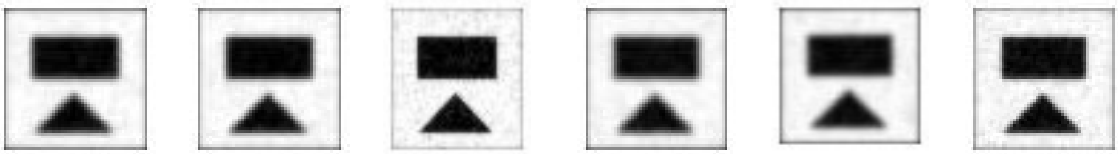

Figure 2. Denoised Images with λ =0.01、0.1、1 (from left to right), where the Iterative Number is 5 using Dirichlet BCs

Table 2. SNR using Periodic BCs

λ	explicit scheme	semi-implicit scheme
0.01	5.8481	6.5320
0.1	5.8659	6.6235
1	5.8640	6.7120

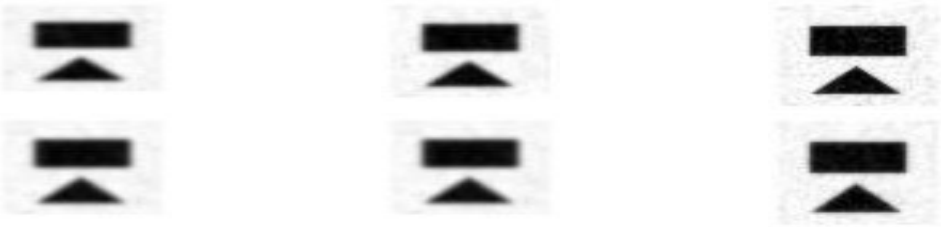

First row: semi-implicit scheme. Second row: explicit scheme

Figure 3. Denoised Images with λ =0.01、0.1、1 (from left to right), where the Iterative Number is 5 using Periodic BCs

Table 3. SNR using Neumann BCs

λ	explicit scheme	semi-implicit scheme
0.01	5.9644	6.6371
0.1	5.7625	6.7484
1	6.1594	6.8396

First row: semi-implicit scheme. Second row: explicit scheme

Figure 4. Denoised Images with λ =0.01、0.1、1 (from left to right), where the Iterative Number is 5 using Neumann BCs

Table 4. SNR using Anti Reflective BCs

λ	explicit scheme	semi-implicit scheme
0.01	6.0014	6.6570
0.1	5.8645	6.8484
1	6.2503	6.9312

First row: semi-implicit scheme. Second row: explicit scheme

Figure. 5 Denoised images with λ =0.01、0.1、1 (from left to right), where the Iterative Number is 5 using Anti Reflective BCs

From the data of Table 1 and Table 4, we can find that all the values of SNR using the semi-implicit scheme are larger than that of using the explicit scheme, respectively. On the other hand, the values of SNR in Table 1, Table 2 and Table 3 also show that the results of the Neumann BCs are better than that of the Dirichlet BCs and the periodic BCs, respectively. Visually, the boundary in Figure 2 has a serious distortion because of Dirichlet BCs, but the Neumann BCs and antireflective BCs can better preserve boundary continuity of the image in Figure 3, Figure 4 and Figure 5. The parameter λ impacts the denoised image greatly. The larger the value of λ, the clearer the denoised image. On the other hand, the smaller the value of λ, the smoother the denoised image.

4. Conclusion

In this paper, a new semi-implicit C-N scheme different from the general explicit scheme is firstly proposed to discrete the famous ROF model. The denoised problem is written as a linear algebra equation problem. The G-S iterative method is used to solve the different linear equations with the five different kinds of BCs--Dirichlet BCs, periodic BCs, Neumann BCs, antireflective BCs and mean BCs. The numerical results show that the semi-implicit discrete scheme gets the larger value of SNR than the explicit scheme, and can better maintain the fine scale features.

References

[1] Rudin L, Osher S, Fatemi E. Nonlinear Total Variation Based Noise Removal Algorithms. *Physica D: Nonlinear Phenomena*. 1992; 60(1-4): 259-268.
[2] Vese LA, Osher SJ. Modeling Textures with Total Variation Minimization and Oscillating Patterns in Image Processing. *Journal of Scientific Computing*. 2003; 19(1-3): 553-572.
[3] Crank J, Nicolson P. *A Practical Method for Numerical Evaluation of Solutions of Partial Differential Equations of the Heat Conduction Type*. Mathematical Proceedings of the Cambridge Philosophical Society. London. 1947; 43: 50-67.
[4] Kim S. PDE-Based Image Restoration: A Hybrid Model and Color Image Denoising. *IEEE Transactions on Image Processing.* 2006; 15(5): 1163-1170.
[5] Wang W, Shi YY. *An Image Denoising Algorithm in the Matrix Form*. The 2nd International Conference on Multimedia Technology (ICMT2011), Hangzhou. 2011: 26-28.
[6] Kim H, Calvert VR, Kim S. Preservation of Fine Structures in PDE-based Image Denoising. *Advances in Numerical Analysis*. 2012; 2012(5): 1-19.
[7] Rosman G, Dascal L, Tai XC, Kimmel R. On Semi-implicit Splitting Schemes for the Beltrami Color Image Filtering. *Journal of Mathematical Imaging and Vision*. 2011; 40(2): 199-213.
[8] Niang O, Thioune A, Gueirea MCE, Delechelle E, Lemoine J. Partial Differential Equation-based Approach for Empirical Mode Decomposition: Application on Image Analysis. *IEEE Transactions on Image Processing.* 2012; 21(9): 3991-4001.
[9] Sun J, Wang Y, Wu XH, Zhang XD, Gao HY. A New Image Segmentation Algorithm and it's Application in Lettuce Object Segmentation. *TELKOMNIKA Indonesian Journal of Electrical Engineering*. 2012; 10(3): 557-563.
[10] Swastika W, Haneishi H. Compressed Sensing for Thoracic MRI with Partial Random Circulant Matrices. *TELKOMNIKA Indonesian Journal of Electrical Engineering.* 2012; 10(1): 147-154.
[11] Shi YY, Chang Q. Acceleration Methods for Image Restoration Problem with Different Boundary Conditions. *Applied Numerical Mathematics.* 2008; 58(5): 602-614.
[12] Strange G. On the Construction and Comparison of Difference Schemes. *SIAM Journal on Numerical Analysis.* 1968; 5(3): 506-517.